J|A|C|S
COMMUNICATIONS

Published on Web 04/01/2006

Force-Induced Insulin Dimer Dissociation: A Molecular Dynamics Study

Taeho Kim, Alexander Rhee, and Christopher M. Yip*

Chemical Engineering & Applied Chemistry, Institute of Biomaterials & Biomedical Engineering, and The Terrence Donnelly Centre for Cellular and Biomolecular Research, University of Toronto, 160 College Street, Toronto, ON, Canada M5S 3E1

Received January 31, 2006; E-mail: christopher.yip@utoronto.ca

A 5.8 kDa dual-chain hormone, insulin must dissociate from its hexameric storage form through an intermediate dimer state to the bioactive monomer before binding to its transmembrane insulin receptor. Understanding the forces and dynamics of insulin dissociation is therefore critical for devising formulations for the treatment of insulin-dependent diabetes. Previous studies have demonstrated that the residues for the β-sheet in the C-terminus of the insulin B-chain are critical for stabilizing the insulin dimer through inter-monomer hydrogen bonding and hydrophobic interactions.[1−6] Especially, dimer dissociation involves disruption of a two-stranded antiparallel β-sheet in the extended C-terminal ends of the B-chain. Persistent inter-monomer hydrogen bonding and hydrophobic interactions exist between residues Phe B24 and Tyr B26 of each monomer at the monomer−monomer interface.[6] Recently, molecular dynamics simulations of the insulin dimer have shown that its structural stability is due, in part, to nonbonded correlated molecular motion.[4] Controlling insulin self-association through site-specific modifications to the dimer-forming region has been a successful strategy for the development of bioactive monomeric insulin analogues.[5,7−9]

We previously applied AFM-based force spectroscopy using covalently tethered and oriented insulin monomers to assess the effect of molecular orientation on insulin−insulin binding forces.[10] Our experimental data suggested that insulin dimer dissociation occurred near the limit of extensibility of the B-chain and that the insulin−insulin interactions across the monomer−monomer interface are stronger than interactions within each monomer. Computational simulations of our study by Clementi et al. using an off-lattice statistical mechanics model provided compelling evidence of this dissociation mechanism.[11]

To provide molecular-level insights into the dynamics of insulin dimer dissociation, steered molecular dynamics (SMD) simulations of the AFM force spectroscopy experiment were performed. All simulations were conducted on the crystallographic insulin dimer (4ins.pdb) using GROMACS 3.2.1 and the GROMOS96 ffG43a1 force field.[13] In these initial studies, a harmonic spring potential was applied to only the C_α of Phe B1 of Monomer I (I:PheB1), while C_α of Phe B1 of Monomer II (II:PheB1) remained fixed (Figure 1). To investigate whether the dissociation pathways and/or dynamics were rate-dependent, SMD experiments were performed at pull rates ranging from 0.0025 to 0.01 nm/ps. In several simulations, the final separation event occurred when each monomer was fully extended with an end-to-end (I:PheB1−II:PheB1) C_α separation of ∼20 nm (Figures 2A and S2). These results are qualitatively consistent with our previous AFM-based force spectroscopy data.[10]

Previous work has demonstrated the importance of intra-monomer ionic (A1:B30, A21:B22) and hydrogen bonding (A11:B4, A21:B23) and inter-monomer hydrogen bonding (B24::B26) to dimer stability.[4] Close inspection of our SMD data revealed

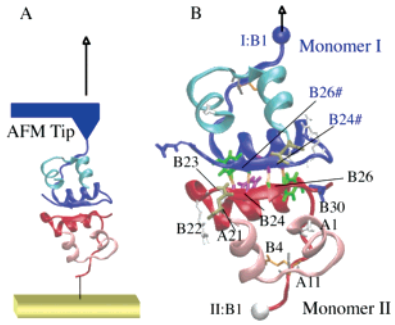

Figure 1. (A) Schematic model of AFM experiment.[10] (B) Molecular model of the insulin dimer. A harmonic spring potential is applied to the C_α of Monomer I at B1 (I:PheB1) (A-chain in cyan; B-chain in blue), while Monomer II (A-chain in pink; B-chain in red) remains fixed to the surface via the C_α of Phe B1 (II:PheB1). Residues involved in specific monomer−monomer interactions are labeled. Hydrogen bonds at the inter-monomer interface are shown as orange dotted lines. Models prepared using VMD.[12]

that, upon application of the external force at I:PheB1, large conformational changes occurred first near the N-terminus of the insulin B-chain of Monomer I (B1−B8), while the α-helical (B9−B19) and the antiparallel β-sheet (B24−B26) regions remained largely unchanged (Figure 2A,E). This was not unexpected since structural changes in residues B1−B8 in part differentiate the insulin R- and T-state conformers.[6] Continued application of external forces led to "unhinging" of the insulin B-chain in the β-turn region (B20−B23) and alignment of the insulin dimer in the pulling direction. This was followed by loss of intra-monomer ionic and hydrogen bonding interactions. The resulting open C-terminus conformation is similar to that reported for the Gly B24 insulin mutant.[5] Subsequent unfolding of the B-chain α-helix led to unraveling of the A-chain α-helix (A13−A19), which is linked to the B-chain by two interchain disulfide linkages. Our simulations suggest that the final stage of dimer separation involves the antiparallel β-strands of each monomer sliding past each other (Figure 2A and Figure 3). The appearance of multiple unbinding events in the simulation data may be due to the formation of transient inter-monomer hydrogen bonds during this slippage phase. In addition, the closely packed residues (B24−B26) enhance the inter-monomer interactions, indicating the importance of hydrophobic interaction. We note that concurrent rupture of multiple bonds has been shown to require a higher force than sequential single bond failure.[14,15]

Not unexpectedly, there are differences between the computational and experimental force curve profiles that are largely a consequence of the computationally inaccessible time scales and pulling rates associated with the real-world experiment (AFM, $\sim 10^{-10}$ nm/ps; SMD, ∼0.005 nm/ps). We note, however, that the computed maximum unbinding force scaled with pulling rate and was also dependent on the dissociation pathway.[16,17]

Our SMD simulations revealed the existence of several unfolding pathways (Figure 2). This was not unexpected since it is well-

10.1021/ja0607382 CCC: $33.50

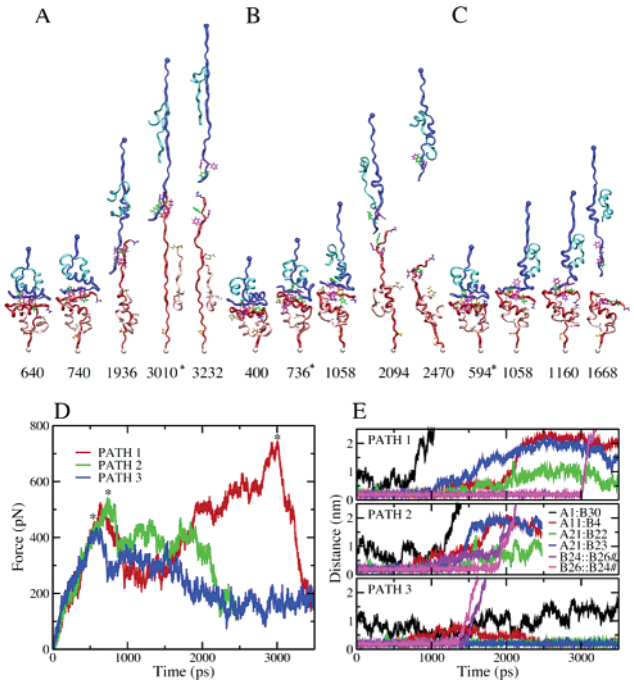

Figure 2. Snapshots of the time-dependent dimer conformation for three different unfolding pathways at a simulated pull rate of 0.005 nm/ps. Water not shown for clarity. Numbers denote elapsed time in picoseconds. (A) PATH 1, (B) PATH 2, (C) PATH 3; ∗ denotes the maximum unbinding force. (D) Corresponding force curves of A, B, and C. (E) Calculated interatom distances in Monomer II residues involved in intra-monomer nonbonded interactions. A1:B30 denotes the distance between A1 N-terminus and B30 C-terminus. A11:B4 and A21:B23 denote the distance of hydrogen bonds between A11 and B4, and A21 and B23, respectively. A21:B22 denotes the distance of the salt bridge between A21 and B22. Inter-monomer interactions (B24::B26#, B26::B24#) are measured by the distance of hydrogen bonding between Monomer I (B24, B26) and Monomer II (B26#, B24#), respectively.

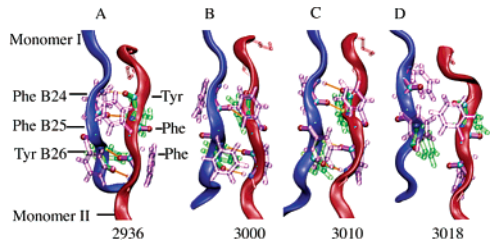

Figure 3. Representative snapshots taken from PATH 1 (Figure 2A,D) at time (A) 2936, (B) 3000, (C) 3010 (maximum unbinding force), and (D) 3018 ps at monomer−monomer interface. B-chain of Monomer I (blue) and Monomer II (red) and important residues (Phe B24 and B25 in purple; Tyr B26 in green) for hydrophobic interactions and hydrogen bonding (orange) are shown in ribbon and licorice representation, respectively.

understood that force spectroscopy probes an energy landscape and that bond strengths are loading rate-dependent.[16] In all cases, dissociation involved unhinging of Monomer I at the β-turn prior to separation of the dimer. Since our SMD studies involved forces applied to only I:PheB1 with loads transduced down the backbone of Monomer I, it is reasonable to expect that the greatest structural changes would occur to Monomer I. This is consistent with the observed dissociation pathways and the role of those residues (A1:B30, A21:B22/B23, B24:B26) involved in stabilizing the intra- and inter-monomer interfaces (Figure 2). These data suggest that the insulin dimer dissociation pathway depends on the relative strength of the inter-monomer interactions across the antiparallel β-sheet interface and the intra-monomer interactions. We note that the α-helical regions defined by residues A1−A8, A13−A19, and B9−B19 are largely unaffected by the dissociation process (Figure 2B,C), and that, after dimer separation, Monomer II undergoes restructuring. Our simulation results strongly support the design of bioactive insulin analogues that involves altering hydrogen bonding and hydrophobic interactions across the β-sheet dimer interface.

In summary, our SMD simulations of force-induced insulin dimer dissociation are in qualitative agreement with our previous AFM study. We have found that the force-induced dissociation of the insulin dimer is a rate- and pathway-dependent process, involving significant conformational changes to the monomer(s). In particular, the relative strength of the inter-monomer interactions across the antiparallel β-sheet interface and intra-monomer interactions of A1 and A30 with B-chain plays critical roles in determining the onset of conformational changes during dissociation. We are currently investigating the effect of known sequence modifications to the insulin dimer-forming region on the forced unfolding pathway and the energetic differences associated with these alterations.

Acknowledgment. We acknowledge support from CIHR, NSERC, the Canada Research Chairs program, and Eli Lilly & Co. T.K. acknowledges CIHR, Institute of Genetics for a Short-term Research Visit grant to visit Dr. Peter Tieleman's Group at University of Calgary. We thank Professor Cecil C. Yip for helpful discussions.

Supporting Information Available: Detailed methods and simulation results (Figures S1 and S2). This material is available free of charge via the Internet at http://pubs.acs.org.

References

(1) Jorgensen, A. M.; Kristensen, S. M.; Led, J. J.; Balschmidt, P. *J. Mol. Biol.* **1992**, *227*, 1146−1163.
(2) Knegtel, R. M.; Boelens, R.; Ganadu, M. L.; Kaptein, R. *Eur. J. Biochem.* **1991**, *202*, 447−458.
(3) Mark, A. E.; Berendsen, H. J.; van Gunsteren, W. F. *Biochemistry* **1991**, *30*, 10866−10872.
(4) Zoete, V.; Meuwly, M.; Karplus, M. *J. Mol. Biol.* **2004**, *342*, 913−929.
(5) Hua, Q. X.; Shoelson, S. E.; Kochoyan, M.; Weiss, M. A. *Nature* **1991**, *354*, 238−241.
(6) Baker, E. N.; Blundell, T. L.; Cutfield, J. F.; Cutfield, S. M.; Dodson, E. J.; Dodson, G. G.; Hodgkin, D. M.; Hubbard, R. E.; Isaacs, N. W.; Reynolds, C. D.; Sakabe, K.; Sakabe, N.; Vijayan, N. M. *Philos. Trans. R Soc. London B Biol. Sci.* **1988**, *319*, 369−456.
(7) Brems, D. N.; Alter, L. A.; Beckage, M. J.; Chance, R. E.; DiMarchi, R. D.; Green, L. K.; Long, H. B.; Pekar, A. H.; Shields, J. E.; Frank, B. H. *Protein Eng.* **1992**, *5*, 527−533.
(8) Richards, J. P.; Stickelmeyer, M. P.; Flora, D. B.; Chance, R. E.; Frank, B. H.; DeFelippis, M. R. *Pharm. Res.* **1998**, *15*, 1434−1441.
(9) Brange, J.; Ribel, U.; Hansen, J. F.; Dodson, G.; Hansen, M. T.; Havelund, S.; Melberg, S. G.; Norris, F.; Norris, K.; Snel, L.; Sørensen, A. R.; Voigt, H. O. *Nature* **1988**, *333*, 679−682.
(10) Yip, C. M.; Yip, C. C.; Ward, M. D. *Biochemistry* **1998**, *37*, 5439−5449.
(11) Clementi, C.; Carloni, P.; Maritan, A. *Proc. Natl. Acad. Sci. U.S.A.* **1999**, *96*, 9616−9621.
(12) Humphrey, W.; Dalke, A.; Schulten, K. *J. Mol. Graphics* **1996**, *14*, 33−38.
(13) Lindahl, E.; Hess, B.; van der Spoel, D. *J. Mol. Model* **2001**, *7*, 306−317.
(14) Gräter, F.; Shen, J.; Jiang, H.; Gautel, M.; Grubmüller, H. *Biophys. J.* **2005**, *88*, 790−804.
(15) Brockwell, D. J.; Paci, E.; Zinober, R. C.; Beddard, G. S.; Olmsted, P. D.; Smith, D. A.; Perham, R. N.; Radford, S. E. *Nat. Struct. Biol.* **2003**, *10*, 731−737.
(16) Merkel, R.; Nassoy, P.; Leung, A.; Ritchie, K.; Evans, E. *Nature* **1999**, *397*, 50−53.
(17) Izrailev, S.; Stepaniants, S.; Balsera, M.; Oono, Y.; Schulten, K. *Biophys. J.* **1997**, *72*, 1568−1581.

JA0607382